

Gas-phase Interaction of Thiophene with the $\text{Ti}_8\text{C}_{12}^+$ and Ti_8C_{12} Met-Car Clusters

Ping Liu,^{*,†} James M. Lightstone,^{†,‡} Melissa J. Patterson,^{†,‡} José A. Rodriguez,[†]
James T. Muckerman,[†] and Michael G. White^{†,‡}

Chemistry Department, Brookhaven National Laboratory, Upton, New York 11973, Department of Chemistry,
SUNY Stony Brook, Stony Brook, New York 11794

Received: January 17, 2006; In Final Form: February 28, 2006

The reactivity of the $\text{Ti}_8\text{C}_{12}^+$ met-car cation toward thiophene was investigated using density functional theory (DFT) and mass selective ion chemistry. It is shown that the experimentally observed mass spectrum can be well described by the DFT calculations. In contrast to the weak bonding interactions seen for thiophene on a $\text{TiC}(001)$ surface, the $\text{Ti}_8\text{C}_{12}^+$ met-car cation is able to interact strongly with up to four thiophene molecules with the cluster staying intact. In the most stable conformation, the thiophene molecules bond to the four low-coordinated Ti^0 sites of $\text{Ti}_8\text{C}_{12}^+$ via a $\eta^5\text{-C,S}$ coordination. The stability and the activity of the $\text{Ti}_8\text{C}_{12}^+$ met-car is observed to increase with an increasing number of attached thiophene molecules at the Ti^0 sites, which is associated with a significant transfer of electron density from thiophene to the cluster. The additional electron density on the $\text{Ti}_8\text{C}_{12}^+$ cation cluster, however, is not sufficient to cleave the C–S bonds of thiophene and the dissociation reaction of thiophene is predicted to be a highly activated process. By contrast, DFT calculations for the neutral Ti_8C_{12} met-car predict that the dissociation reaction leading to adsorbed S and C_4H_4 fragments is energetically favorable for the first thiophene molecule. The binding behavior for subsequent addition of thiophene molecules to the neutral met-car is also presented and compared to that of the cation.

I. Introduction

Since their discovery by Castleman and co-workers in 1991,¹ the M_8C_{12} metalcarbohedrene (met-car) clusters of the early transition metals ($\text{M} = \text{Ti}, \text{Zr}, \text{V}, \dots$) and their building blocks have attracted significant interest due their high stability, unique structure, and electronic properties.^{2–5} The remarkable stability of the met-car clusters has been attributed to their compact, cage-like structure. For the met-car Ti_8C_{12} , a pentagonal dodecahedral T_h structure (Figure 1a) was originally proposed by Castleman and co-workers.¹ Recently, most theoretical^{3,6} and experimental^{7–9} results agree on a tetrahedral structure with near- T_d symmetry. We have found by using both density functional theory (DFT) and ab initio quantum chemistry (MP2, MP4, and QCISD) that the Ti met-car energetically prefers slightly distorted near- T_d symmetry (D_{2d} or C_i), with four low-coordinated metal atoms (Ti^0 in Figure 1b) and four high-coordinated metal atoms (Ti^I in Figure 1b) arranged in two near-tetrahedra and interconnected by six C_2 groups.^{3,4,10–13} Calculations have also shown these C_2 groups act as “reservoirs” of negative charge.^{10,11} These unique structural and electronic properties allow the met-car to interact with and bind molecules by acting as both an electron acceptor and donor through facile charge transfer at the low coordinated metal sites.^{10,11,14,15}

Metal carbides in bulk form display a superior ability to catalyze many hydrogen transfer and hydrotreating reactions.^{16,17} The met-car clusters, with their uniform size and characterizable active sites, are interesting model systems for exploring the effects of size and composition (C/M ratio) on chemical reactivity. Previously, we calculated the energetics of CO, SO_2 , H_2O , and NH_3 adsorption on several M_8C_{12} ($\text{M} = \text{Ti}, \text{V}, \text{Mo}$)

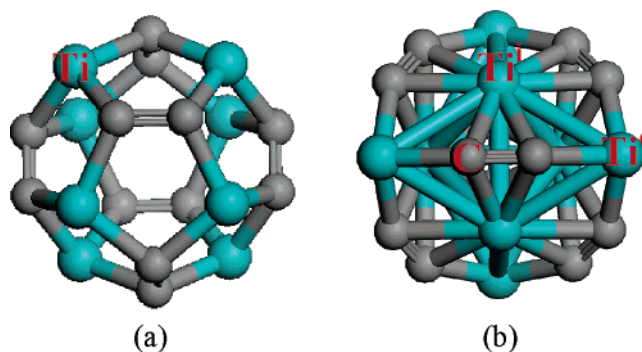


Figure 1. Optimized configuration of a Ti_8C_{12} met-car with T_h (a) and near- $T_d\text{-}C_i$ (b) symmetry.

neutral clusters,^{10,11,18,19} or OCS, CS_2 , and SO_2 on $\text{Ti}_8\text{C}_{12}^+$,¹⁵ showing that the met-car can behave differently than bulk metal carbides. Despite a high C/M ratio, M_8C_{12} clusters display a reactivity intermediate between those of bulk M_2C and MC surfaces. Experimental validation of the aforementioned calculations, however, is not possible with isolated, neutral met-car clusters, but mass-selected beams of met-car cations (or anions) are readily produced by gas-phase cluster sources. The reactivity of the charged clusters can be explored using low-pressure collision cells and mass spectrometry.^{2–4,15} In the 1990s, Castleman and co-workers employed these methods to investigate the gas-phase interaction of $\text{Ti}_8\text{C}_{12}^+$ with a number of molecules such as methanol, water, ammonia, benzene, pyridine, and ethylene.^{20,21} Different reactivity patterns were observed for π -bonding molecules (benzene, pyridine, and ethylene) whose binding to the met-car cation would truncate at four ligands, while interactions with polar molecules (methanol, water, and ammonia) lead to the binding of eight ligands.

* Corresponding author e-mail: pingliu3@bnl.gov.

[†] Brookhaven National Laboratory.

[‡] SUNY Stony Brook.

It was also observed that for the same truncation, the distribution of the peak intensity varies with the different molecules. For instance, with the successive addition of molecules, the intensities of the adsorption peaks increase in the case of homocyclic benzene, and they decrease for heterocyclic pyridine. These observations were interpreted in the previous studies^{20,21} on the basis of the wrong (T_h) structure of the met-car (Figure 1a), where the polar molecules were thought to bind to each of eight equivalent Ti atoms and the π -bonded molecules to bridge-bond between two adjacent Ti atoms. Since then, several theoretical studies have been carried out to interpret the interactions of Ti_8C_{12} with polar molecules (ammonia and water) using the now generally accepted T_d or near- T_d structure for the met-car.^{11,22} Among the π -bonding molecules, only the interaction with benzene has been investigated theoretically.²² None of these theoretical studies, however, deals with the $Ti_8C_{12}^+$ cation, or involves the sequential adsorption of the molecule by the met-car to reproduce the experimental observations, both aspects are very important for understanding the reactivity of the met-car cluster.

One of the purposes of the present study is to gain a better understanding of the surface reactivity of the met-car cluster with π -bonding molecules. Thiophene can bind to metal centers though its S lone pair or its aromatic ring. A priori, it is not clear how a ligand with such properties will behave when reacting with Ti_8C_{12} or $Ti_8C_{12}^+$. In addition, this work is also motivated by our recent calculations showing that the Ti_8C_{12} met-car is able to act as a catalyst for the complete reaction cycle required for the hydrosulfurization (HDS) of thiophene,¹⁴ a prototypical reaction often used to test for HDS activity.^{16,17} The results presented here show that the experimentally observed probabilities for the sequential interaction of thiophene with $Ti_8C_{12}^+$ can be well described by DFT calculations. For comparative purposes, DFT calculations are also presented for thiophene interactions with the neutral Ti_8C_{12} met-car cluster. Our theoretical studies are able to give, for the first time, a clear explanation for the pattern seen for the sequential reactivity of π -bonding cyclic molecules with met-car clusters.

II. Methods

II.A. Experiment. The work presented here was performed on a newly constructed cluster apparatus that is capable of investigating the gas-phase reactivity of cluster ions using mass spectrometry to isolate the cluster ion of interest and analyze the products resulting from reactive collisions. The details of the apparatus and the experimental procedure will be published elsewhere.¹⁵ Briefly, a magnetron sputtering source (Oxford, NC200U) is used to generate $Ti_xC_y^+$ clusters by reactive sputtering of a titanium metal target with a gas mixture of 2% CH_4 in Ar. A single cluster mass, e.g., $Ti_8C_{12}^+$, is selected by its m/z ratio by a downstream quadrupole mass filter (ABB Extrel) and then transmitted into a hexapole ion-guide that includes an enclosed collision cell for the introduction of collision/reaction gases. A mixture of 1% thiophene in He was introduced into the collision cell using a variable leak valve with the pressure (~ 10 mTorr) measured by a capacitance manometer (MKS). The products were mass analyzed by a second quadrupole mass spectrometer (Extrel) located downstream of the ion-guide and detected by a channeltron electron multiplier. All experiments were carried out at room temperature.

II.B. Theory. Calculations based on density functional theory (DFT) were used to study the interaction of thiophene with the $Ti_8C_{12}^+$ cation and neutral Ti_8C_{12} met-cars. The calculations

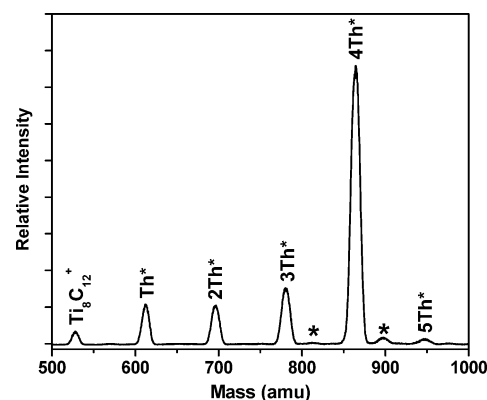


Figure 2. Mass spectra of the products resulting from the adsorption of thiophene with the $Ti_8C_{12}^+$ met-cars. X* corresponds to an adsorbed X species.

were performed with the DMol³ code, which allows modeling the electronic structure and energetics of molecules, solids, and surfaces using DFT.^{23,24} Here, all the electrons of C, H, S, and Ti were included explicitly, instead of replacing core electrons by a single effective potential (effective core potential). A numerical basis set was employed, which describes the orbitals in the valence shell with double numerical functions and includes a polarization d-function for the light atoms (for example, C: 1s 2s 2p 2s' 2p' 3d). It is comparable in accuracy to a Gaussian 6-31G* basis set. A local basis cutoff of 5.5 Å in real space was employed. When a more extended basis set and a higher cutoff were tested, no remarkable changes resulted. The generalized gradient approximation (GGA), with the revised version of the Perdew–Burke–Ernzerhof (RPBE) functional,²⁵ was used in the present work. The spin-unrestricted and spin-restricted calculations were performed for $Ti_8C_{12}^+$ and Ti_8C_{12} , respectively. Our previous study using relatively high-level theories such as MP2, MP4, and QCISD as well as DFT showed that the ground state of Ti_8C_{12} is a closed shell,¹¹ while a doublet was found for the cation. No spin change was found when the met-cars adsorb and dissociate thiophene. The geometries for both the adsorbate and the met-car systems were optimized with no symmetry constraints. Our calculations show that by losing one electron, $Ti_8C_{12}^+$ is 4.56 eV less stable than Ti_8C_{12} , which agrees well with the experimental (4.40 ± 0.02 eV)⁴ and other theoretical (4.47 eV) studies.²⁶ Earlier studies using the same theoretical approach employed here were very useful for examining the bonding of CO, S, CO₂, and thiophene with both metal carbide surfaces and nanoparticles. Calculated adsorption energies were found to be very close ($|\Delta E| < 0.25$ eV) to those measured experimentally or predicted by DFT plan-wave pseudopotential calculations.^{10,18,19,27,28} Transition states here were identified using the combination of synchronous transit methods and eigenvector following,^{29,30} and verified by the presence of a single imaginary frequency from a sequential vibrational frequency analysis.

III. Results and Discussion

Figure 2 displays the experimental mass spectrum for the interaction of thiophene with the $Ti_8C_{12}^+$ met-car. The prominent mass peaks correspond to the formation of cluster adducts with up to four thiophene molecules bonded to the intact met-car cluster. Based on the observed intensity distribution, the met-car bonded to four thiophene molecules ($4Th^*$ in our notation) is the most probable product under our experimental conditions. In contrast, the interaction of the fifth thiophene with $Ti_8C_{12}^+$ ($5Th^*$ in our notation) is apparently much weaker, as evidenced

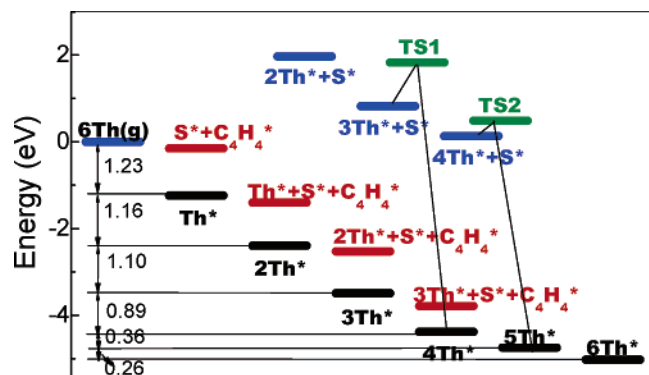


Figure 3. Calculated potential energy diagram for the adsorption of thiophene (Th) with a $\text{Ti}_8\text{C}_{12}^+$ met-car. The energies in the figure are expressed respect to a free $\text{Ti}_8\text{C}_{12}^+$ met-car, and free thiophene molecules in gas phase. X* corresponds to an adsorbed X species. TS stands for the transition state.

by the very small peak at the corresponding mass (948 amu). This is different from results for adsorption of OCS, CS_2 , and SO_2 , where the bonding of at least six molecules to the met-car cation was observed.¹⁵ Two smaller peaks at 812 and 896 amu (marked by asterisks in Figure 2) correspond in mass to $(3\text{Th}^* + \text{S})$ and $(4\text{Th}^* + \text{S})$ products and suggest a decomposition reaction involving a thiophene molecule and the 3Th^* and 4Th^* adducts, respectively. The intensities of these peaks, however, were not found to be reproducible under all experimental conditions and are tentatively attributed to impurities in the thiophene sample or from the sample inlet system.

DFT calculations were performed to understand the cluster product peak intensities in the experimental mass spectrum (Figure 2). Figures 3 and 4 display, respectively, the calculated potential energy diagram and the geometry of some of the cluster products involved in the interaction between thiophene and the $\text{Ti}_8\text{C}_{12}^+$ cluster. The energies in Figure 3 are expressed with respect to the isolated $\text{Ti}_8\text{C}_{12}^+$ cluster and individual thiophene molecules in the gas-phase.

Similar to the case of neutral Ti_8C_{12} (Figure 1b), our calculations show that $\text{Ti}_8\text{C}_{12}^+$ prefers a distorted T_d -like structure with no symmetry (C_1 point group). Comparing Figures 2 and 3, one can see that the trend in stability inferred from the experimental peak intensities is qualitatively reproduced by the DFT calculations. Specifically, we identify a lower total energy with a higher probability for adduct formation which, in turn, should result as a stronger peak in the product mass spectrum.

To put the predicted binding configurations of thiophene on the met-car cluster in context, it should be noted that the coordination mode for thiophene on extended metal carbide surfaces and inorganic complexes strongly depends on the composition of the systems. On the surfaces of transition metals and metal-terminated metal carbides with a carbon/metal ratio of 0.5, an $\eta^5\text{-S,C}$ (one S and four C bonding with the metals) mode is preferred, which is accompanied by a spontaneous cleavage of the C–S bond.^{18,31} An $\eta^3\text{-S,C}$ (one S and two C bonding with a metal) mode is identified when interacting with inorganic complexes,³² while $\eta^1\text{-S}$ (one S bonding with a metal) becomes favorable when thiophene is adsorbed on the (001) surface of metal carbides with a carbon/metal ratio of 1.¹⁸ Neither the $\eta^3\text{-S,C}$ nor the $\eta^1\text{-S}$ mode leads to the dissociation of thiophene. On $\text{Ti}_8\text{C}_{12}^+$, different adsorption configurations were considered, including the atop adsorption at the low-coordinated Ti^0 and the high-coordinated Ti^i sites in either an $\eta^1\text{-S}$ or an $\eta^5\text{-S,C}$ mode. It was found that a thiophene molecule prefers to bond to $\text{Ti}_8\text{C}_{12}^+$ molecularly at a Ti^0 site in the $\eta^5\text{-$

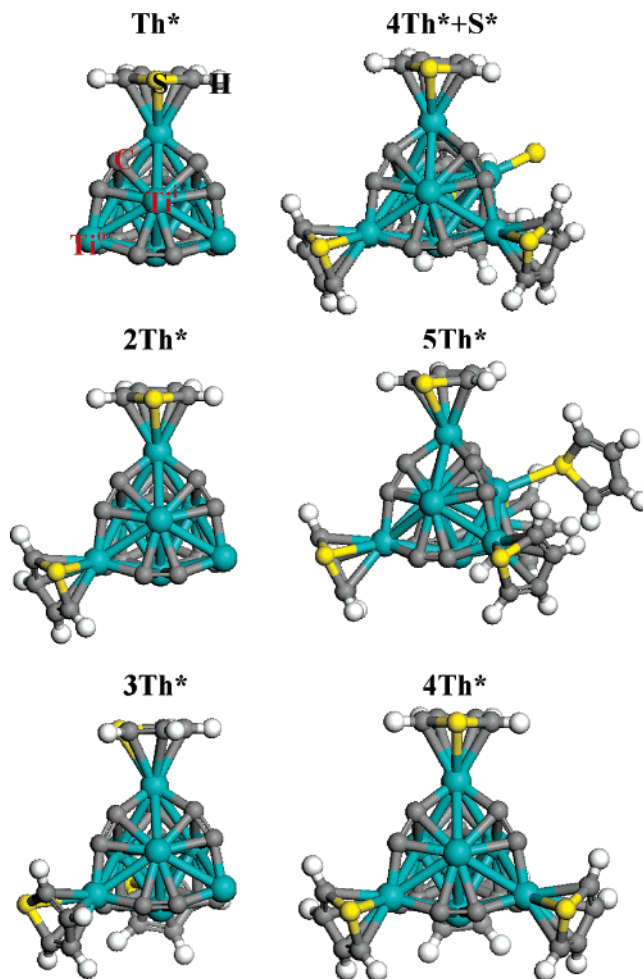


Figure 4. Optimized geometries of some of the products involved in the interaction of thiophene (Th) with a $\text{Ti}_8\text{C}_{12}^+$ met-car. X* corresponds to an adsorbed X species.

TABLE 1: Calculated Parameters for Thiophene Adsorption on a $\text{Ti}_8\text{C}_{12}^+$ Met-Car^a

	$d(\text{Ti}-\text{S})$ (Å)	$d(\text{Ti}-\text{C})$ (Å)	$d(\text{C}-\text{S})$ (Å)	$\theta(\text{C}-\text{S}-\text{C})$ (°)
Th_{gas}			1.74	91.64
Th^*	2.72	2.55~2.57	1.75	91.00
2Th^*	2.72	2.55~2.57	1.76	90.95
3Th^*	2.71	2.55~2.57	1.76	90.84
4Th^*	2.71	2.55~2.57	1.76	90.81
5Th^*	2.71	2.55~2.57	1.76	90.80
	2.86		1.74	92.02

^a The geometries of $n\text{Th}^*$ are shown in Figure 4, where most of Th molecules prefer the Ti^0 sites of the met-car. In the case of 5Th^* , one of the Th molecules occupies the Ti^i site, and the corresponding parameters are displayed in italics.

S,C mode (Th^* , Figure 4), with a binding energy of -1.23 eV. The thiophene molecule adsorbed at the Ti^0 sites in the η^1 mode is not stable at all, and transforms to the $\eta^5\text{-S,C}$ mode during the geometry optimization. At the Ti^i sites, however, the $\eta^1\text{-S}$ mode is the more favorable but with a relatively small binding energy of only -0.26 eV. A spontaneous shift from $\eta^5\text{-S,C}$ to $\eta^1\text{-S}$ binding configuration was observed at the Ti^i sites, which we attribute to steric repulsion between the outward-shifted C_2 groups of the met-car and the molecule. As shown in Table 1, the S–C bonds of thiophene are slightly stretched and the C–S–C bond angle is contracted when the molecule is adsorbed at the Ti^0 site.

A similar site preference for the low-coordinated Ti^0 sites has also been found for other molecules (CO , H_2O , NH_3) in

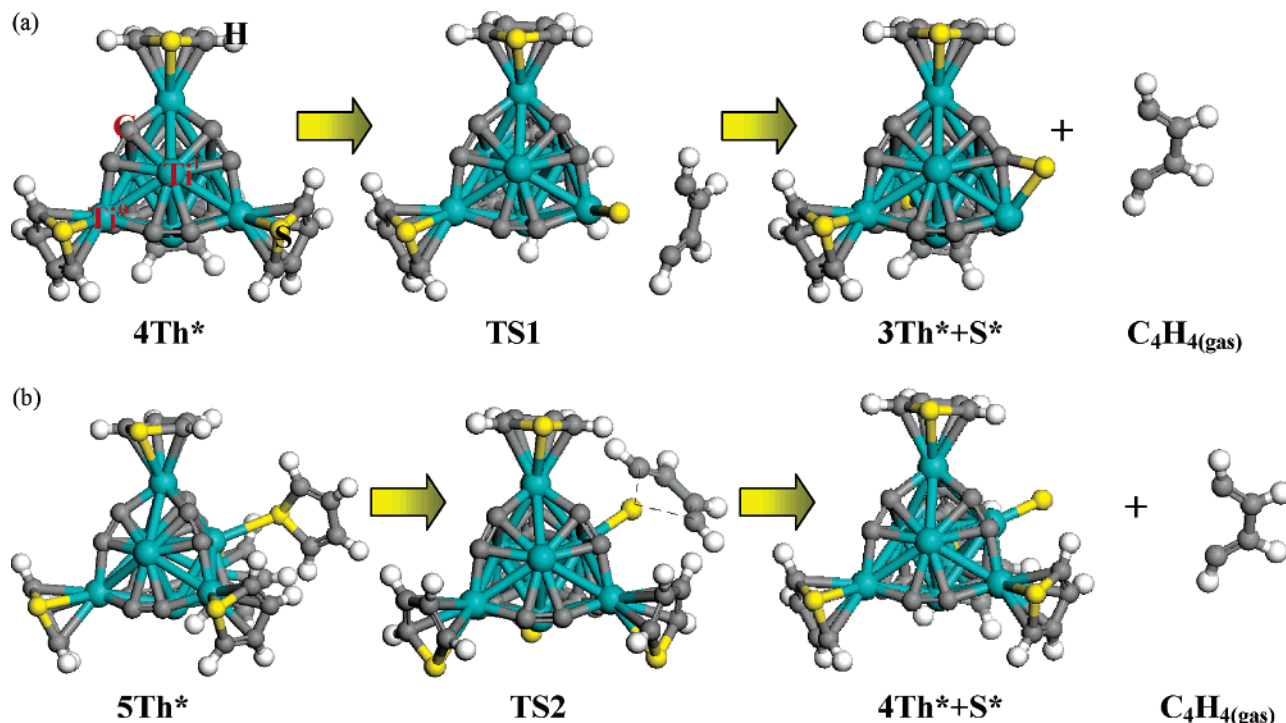


Figure 5. Optimized geometries of the transition states (TS) and the products involved in the dissociation of thiophene (Th) on a $\text{Ti}_8\text{C}_{12}^+$ met-car adsorbing 3 Th molecules ($4\text{Th}^* \rightarrow 3\text{Th}^* + \text{S}^* + \text{C}_4\text{H}_4(\text{gas})$, a) and 4 Th molecules ($5\text{Th}^* \rightarrow 4\text{Th}^* + \text{S}^* + \text{C}_4\text{H}_4(\text{gas})$, b), respectively. X* corresponds to an adsorbed X species.

our previous computational studies of neutral met-car bonding.^{10,11,18,19} By contrast, the binding of thiophene at the Mo^0 sites of the Mo_8C_{12} met-car is slightly more favorable (~ 0.1 eV) in the η^1 -S mode than in the η^5 -S,C mode.¹⁸ The difference is traced to the higher stability of Ti_8C_{12} met-car, which has a calculated formation energy that is lower than that of Mo_8C_{12} by 0.74 eV/atom. The weaker bonding in the Mo_8C_{12} cluster can result in the C_2 groups shifting further outward than those of Ti_8C_{12} . This may lead to a more repulsion between the C_2 groups and thiophene the adsorbed in the η^5 -S,C mode at the Mo^0 sites.

Upon increasing the number of thiophene ligands from one to four, the four Ti^0 sites of $\text{Ti}_8\text{C}_{12}^+$ are occupied sequentially (Figure 4), and the ΔE drops almost linearly to -4.38 eV (4Th^*). This is different from trends seen on surfaces of bulk metal carbides, where a substantial weakening of the interaction between thiophene and the surfaces was observed upon raising the coverage.^{19,25,33} As shown in Figure 3, the energy gains for bonding an extra thiophene molecule, $E[(n+1)\text{Th}^*] - E(\text{Th}) - E(n\text{Th}^*)$, decreases slightly in going from Th^* (-1.23 eV) to 4Th^* (-0.89 eV). One can also see in Table 1 that from Th^* to 4Th^* , the bonding geometry for each thiophene at the Ti^0 site does not seem to change. The addition of a fifth thiophene ligand results in a much smaller energy gain (-0.36 eV), although its calculated total energy (-4.74 eV) is lower than the 4Th^* adduct. The later would be expected to result in 5Th^* having a higher probability for formation than the smaller adducts with 1–4 thiophene molecules. The experimental mass spectrum, however, shows only a very small peak at the mass corresponding to 5Th^* (Figure 2).

To understand this, we have to consider the stability of the adduct formed by the incorporation of a fifth thiophene ligand. As noted above, the energy released by the reaction, $4\text{Th}^* + \text{Th} \rightarrow 5\text{Th}^*$, is only -0.36 eV. This can be attributed to the fact that all the active Ti^0 sites have been occupied in 4Th^* (Figure 4), and the fifth ligand has to interact only through S

(η^1) with the Ti^i sites, which are less reactive than Ti^0 sites.^{10,11,18,19} These results suggest that 5Th^* is not particularly stable with respect to $4\text{Th}^* + \text{Th}$ under the current experimental conditions. As shown in Figure 3, the adsorption of a thiophene ligand results in a substantial energy release that would be converted to internal energy (rovibrational) in the association adducts. In the present experiment, the products are cooled by multiple collisions with background helium gas atoms, which can stabilize the internally “hot” association product. This cooling is apparently effective for the strongly bonded adducts, $1\text{Th}^* - 4\text{Th}^*$, which are the most prominent peaks in the mass spectrum (Figure 2). For 5Th^* , enough internal energy may remain in the “cooled” cluster adduct to break the relatively weaker $\text{Th}-\text{Ti}^i$ bond, so that much of the 5Th^* eventually dissociates to 4Th^* . As a consequence, only a small amount of the 5Th^* product survives experimental detection (Figure 2). Furthermore, the net energy gain for adding a sixth thiophene (-0.26 eV), $5\text{Th}^* + \text{Th} \rightarrow 6\text{Th}^*$, is even less than for 5Th^* (Figure 3). This trend should result in the 6Th^* species having an even lower probability for formation than 5Th^* , consistent with its absence in the experimental spectrum (Figure 2).

We now turn our attention to the dissociation reaction of thiophene on the $\text{Ti}_8\text{C}_{12}^+$ cluster. As shown in Figure 3, we first note that the dissociation adsorption of thiophene, leading to S^* and C_4H_4^* fragments, is energetically less favorable than intact molecular adsorption for all the cases considered ($1\text{Th}^* - 4\text{Th}^*$). In addition, the alternative dissociation reaction in which the S^* atom remains bound to the met-car and the C_4H_4 hydrocarbon fragment is lost to the gas-phase ($\text{Th}^* \rightarrow \text{S}^* + \text{C}_4\text{H}_4(\text{g})$) is highly endothermic ($\Delta E = +5.67$ eV) and energetically infeasible. We also notice that the energetics of the dissociation reaction on $\text{Ti}_8\text{C}_{12}^+$ met-car cation change greatly with an increasing number of adsorbed thiophene molecules. From the calculations, this trend is indicative of changes in electron density and binding energies at the Ti^i sites and the C_2 sites of the met-car cluster. To illustrate this, we used a sulfur

atom as probe, and our DFT results show that compared to a bare $\text{Ti}_8\text{C}_{12}^+$ cluster, the S–Tiⁱ bond is strengthened by 0.17 eV when the met-car adsorbs three thiophene molecules at the Ti⁰ sites. The S–Tiⁱ bond strength increases by an additional 0.40 eV when all four Ti⁰ sites of the $\text{Ti}_8\text{C}_{12}^+$ cluster are occupied by thiophene molecules. Similarly, we find that the binding energies of CO and H₂O at the Tiⁱ sites increase by 0.04 eV and 0.21 eV, respectively, when going from the bare $\text{Ti}_8\text{C}_{12}^+$ cluster to 4Th*.

The question remaining is whether the Tiⁱ sites in 3Th* or 4Th* are active enough to break the C–S bonds of thiophene. The dissociation reaction on 3Th* (Figure 5a), $4\text{Th}^* \rightarrow 3\text{Th}^* + \text{S}^* + \text{C}_4\text{H}_{4(g)}$, is predicted to be highly endothermic ($\Delta E = +5.20$ eV), which corresponds to the transition state, TS1, and a high barrier of 6.21 eV (Figure 3). With one more adsorbed thiophene (4Th*), the Tiⁱ site becomes more active, and ΔE is lowered to 4.88 eV ($4\text{Th}^* + \text{S}^*$) with a barrier of 5.23 eV (Figures 3 and 5b). That is, the dissociation of thiophene on a $\text{Ti}_8\text{C}_{12}^+$ cluster is highly activated and is very unlikely to take place on the bare met-car or any of the $n\text{Th}^*$ met-car adducts. This conclusion supports our earlier contention that the small peaks at 812 and 896 amu are not due to the decomposition of a thiophene molecule on the 3Th* and 4Th* adducts, respectively, despite their mass coincidence. Therefore, even though the activity of the $\text{Ti}_8\text{C}_{12}^+$ cluster increases due to the adsorption of thiophene at the Ti⁰ sites, the cluster–thiophene interaction is not strong enough to drive the dissociation reaction involving the release of the C_4H_4 product.

To understand the behavior of $\text{Ti}_8\text{C}_{12}^+$ toward thiophene, we also calculated the total electron density mapped by the electrostatic potential as shown in Figure 5. The blue corresponds to negatively charged regions, while the red represents positively charged regions. One can see in Figure 6 that all the Ti atoms are positively charged, and the C atoms are negatively charged. The bonding of each thiophene involves a significant transfer of electron density from the ligand to the $\text{Ti}_8\text{C}_{12}^+$ cluster ($0.22e \sim 0.32e$ according to the Mulliken population analysis). On the met-car cation cluster, as shown in Figure 7, each thiophene adsorption involves some donation of electronic charge from the π orbital of thiophene to the vacant d -like orbital of Ti⁰ (known as σ donation). Simultaneously, back-donation moves electronic charge from the occupied d -like orbitals of Ti⁰ to the π^* orbital (i.e., the antibonding π orbital) of thiophene (known as π back-donation). Our results show that σ donation is larger than the π back-donation, and a net transfer of electron density to the $\text{Ti}_8\text{C}_{12}^+$ cation is observed. Figure 7 also indicates that the excess electron density on the Ti⁰ atom bonded with thiophene is partially donated to the neighboring C₂ units and the Tiⁱ atoms through the d orbitals of Ti⁰. Thus, one can see in Figure 6 that in going from Th* to 4Th*, the electron density at the unoccupied Ti⁰ sites hardly changes, and the gradual electron density accumulations at the Tiⁱ sites and the C₂ sites are clearly observable. In fact, this leads to an increased bond strength between the Tiⁱ sites and ligands such as S, CO, and H₂O, according to the present calculations. Yet, as C–S bond cleavage is a highly electron-demanding process,^{18,19,33,34} both our experimental and theoretical results show that even with the electron-enriched Tiⁱ and C₂ sites, the $\text{Ti}_8\text{C}_{12}^+$ cation cannot dissociate thiophene due to a barrier of more than 5 eV.

For purposes of comparison, identical calculations were also carried out for the reaction of thiophene with the neutral Ti_8C_{12} met-car. In general, the calculated potential energy diagram (Figure 8) was found to be similar to that of the $\text{Ti}_8\text{C}_{12}^+$ cation (Figure 3), i.e., it can bind four thiophene molecules with a

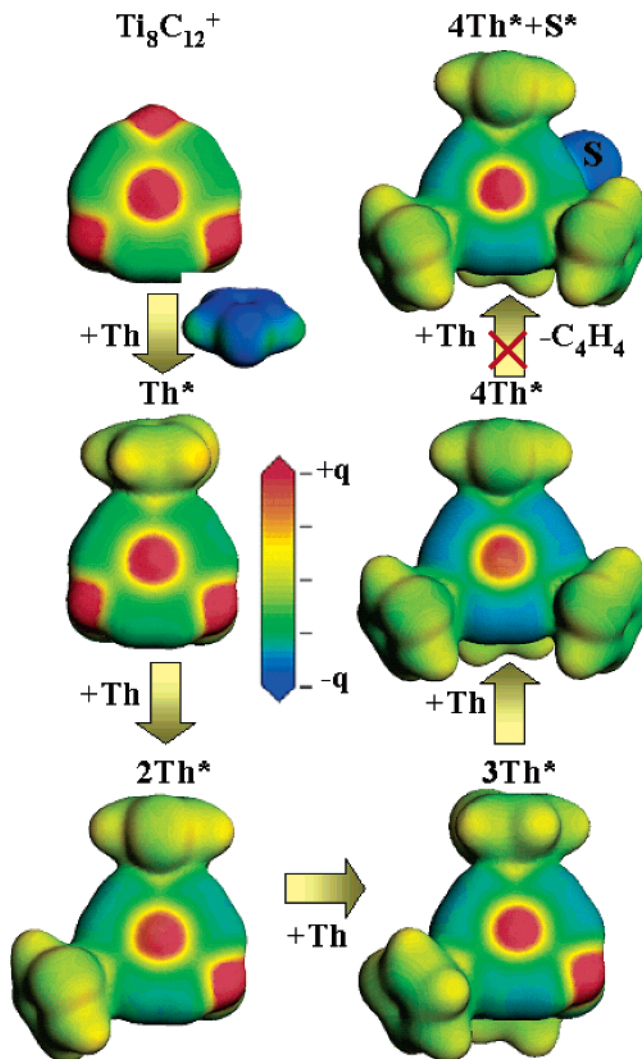


Figure 6. Calculated total electron density mapped by the electrostatic potential of the products in the interaction of thiophene with a $\text{Ti}_8\text{C}_{12}^+$ met-car. The isosurface value is $0.05e \text{ \AA}^{-3}$. Electrostatic potential is color coded as follows: the dark gray (the blue in color) corresponds to negatively charged regions, while the white (the red in color) represents positively charged regions.

substantial energy stabilization (-4.01 eV). However, the adsorption geometries for thiophene are somewhat different. As shown in Figure 8, on the neutral met-car the dissociative adsorption ($\text{S}^* + \text{C}_4\text{H}_4^*$, Figure 9) is more energetically favorable by 0.28 eV than molecular adsorption in the η^5 -S,C mode observed in the case of the cation (Th^* , Figure 4). Since the additional electron in the neutral met-car increases the electron density compared to that of the cation, both the sulfur atom and the hydrocarbon fragment can strongly interact with the neutral Ti_8C_{12} cluster. For the sequential adsorption of the second thiophene, however, adsorption at the Ti⁰ sites via the η^5 -S,C coordination (Figure 9) is preferred over dissociative adsorption. Both the S^* and C_4H_4^* fragments from the dissociation of the first adsorbed thiophene withdraw electron density from the met-car and are negatively charged by $-0.52e$ and $-0.26e$, respectively. As a result, the met-car cannot provide enough electron density to cleave the C–S bonds of the second adsorbed thiophene. Even with the back transfer of electron density from one or two adsorbed thiophene molecules ($\text{Th}^* + \text{S}^* + \text{C}_4\text{H}_4^*$ and $2\text{Th}^* + \text{S}^* + \text{C}_4\text{H}_4^*$, Figure 8) ($\sim 0.18e$ per thiophene), the dissociation of multiple thiophene molecules on Ti_8C_{12} is very unlikely ($2\text{Th}^* + 2\text{S}^* + 2\text{C}_4\text{H}_4^*$, Figure 8)

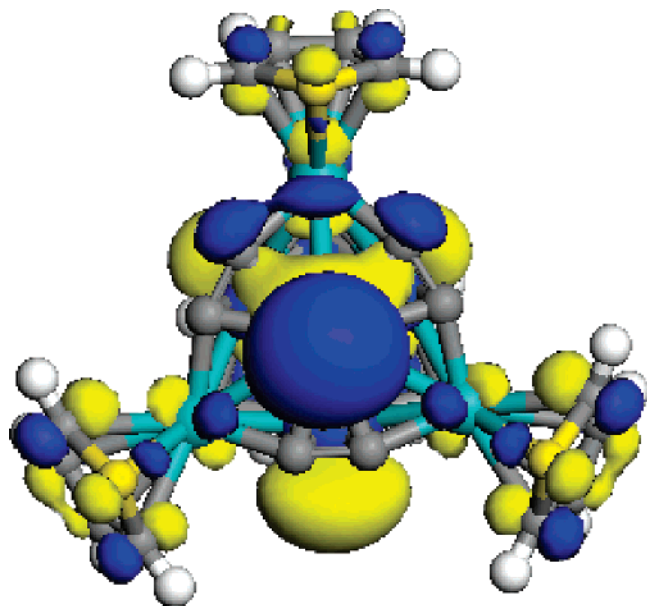


Figure 7. Molecular orbital (HOMO) involved in the σ donation for a $\text{Ti}_8\text{C}_{12}^+$ met-car bound to four thiophene molecules at the Ti^0 sites via the $\eta^5\text{-S,C}$ conformation.

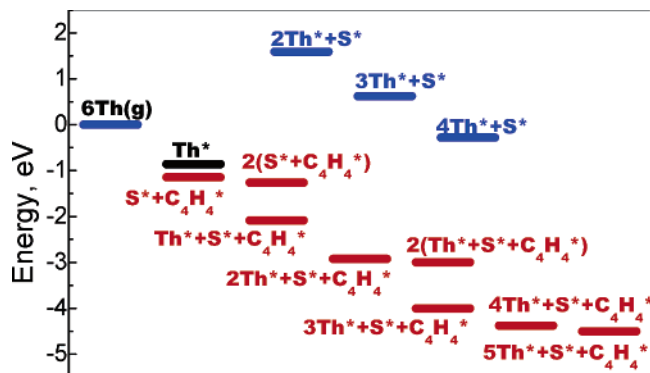


Figure 8. Calculated potential energy diagram for the adsorption of thiophene (Th) by a Ti_8C_{12} met-car. The energies in the figure are expressed with respect to a free Ti_8C_{12} met-car and free thiophene molecules in the gas phase. X^* corresponds to an adsorbed X species.

compared to the adsorption of intact thiophene ($3\text{Th}^* + \text{S}^* + \text{C}_4\text{H}_4^*$). In this way, all Ti^0 sites of Ti_8C_{12} are occupied after interacting with four thiophene molecules (Figure 9). Our calculations also show that a fifth thiophene ligand does not move to a Ti^{I} sit, but rather shares a Ti^0 site with C_4H_4^* via the $\eta^5\text{-S,C}$ coordination, albeit with a small binding energy (-0.38 eV). Repulsion caused by the addition of the fifth thiophene molecule leads to a shift of the C_4H_4^* fragment from a $\text{Ti}^0\text{-C}$ bridge site to one which is more centered on top of the C atom (Figure 9). The addition of a sixth thiophene molecule results in an even smaller binding energy (-0.13 eV) as it occupies the less active Ti^{I} sites via the $\eta^1\text{-S}$ coordination (Figure 8).

As noted above, the dissociation reaction leading to the release of the C_4H_4 fragment into gas-phase, $n\text{Th}^* + \text{S}^* + \text{C}_4\text{H}_4^* \rightarrow n\text{Th}^* + \text{S}^* + \text{C}_4\text{H}_{4(\text{g})}$, is highly activated on the Ti_8C_{12} neutral met-car with $\Delta E > +4.10$ eV. This is due to the fact that the hydrocarbon fragment bonds too strongly to be removed from the met-car. However, as a good catalyst for the HDS reaction, both sulfur and hydrocarbon fragments have to be desorbed from the surface efficiently. According to our previous study,¹⁴ the barrier for the removal of S^* and C_4H_4^* can be lowered greatly

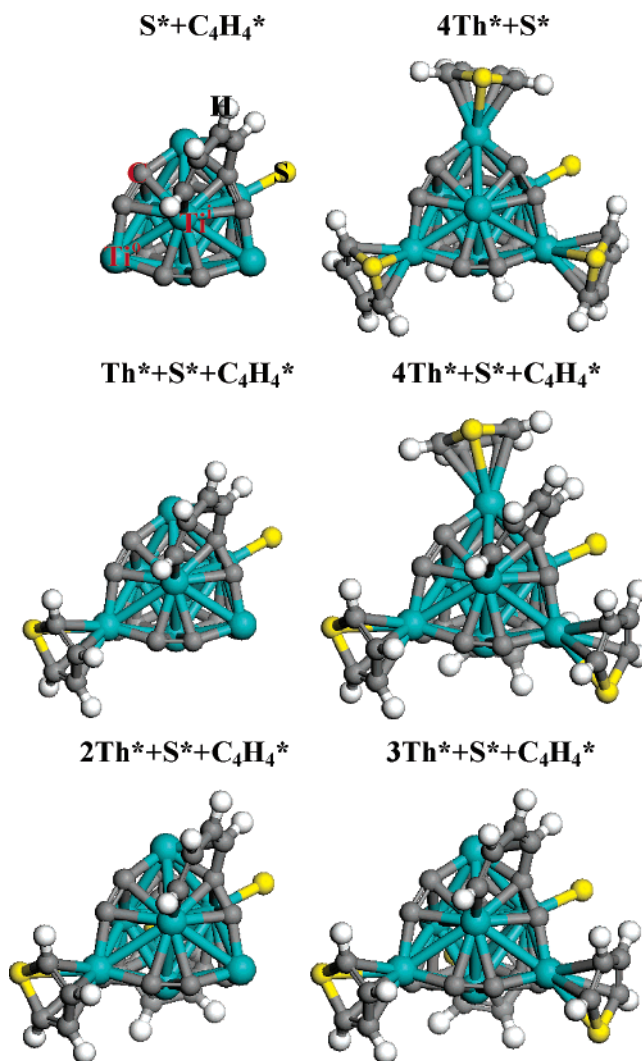


Figure 9. Optimized geometries of some of the products involved in the interaction of thiophene (Th) with a Ti_8C_{12} met-car. X^* corresponds to an adsorbed X species.

by introducing H_2 into the reaction as preadsorbed H atoms. This prediction will be tested experimentally in our further studies.

Overall, our results show that for the reactivity of small clusters such as the Ti met-cars, adsorption of thiophene at high coverage has to be taken into consideration. The reactivity increases with coverage, since the adsorbed thiophene molecules enhance the activity of the Ti^{I} sites and C_2 sites through the transfer of electron density. In addition, we also notice that the behavior of the Ti met-car cation toward thiophene is not necessarily the same seen for the interaction with other π -bonding molecules.²⁰ For instance, although the Ti met-car cation is also able to adsorb up to four pyridine molecules, the intensity of the adsorption peaks does decrease with coverage²⁰ as seen for extended surfaces. The differences in the behavior of thiophene and pyridine could be a consequence of variations in steric repulsion among the bonded ligands, or variations in the extent of the ligand \rightarrow met-car electron transfer. On the other hand, the sequential adsorption of benzene on the Ti met-car cation²¹ shows trends which are very similar to those seen here for the sequential adsorption of thiophene. Theoretical calculations for the sequential adsorption of benzene and pyridine on the Ti met-car cation are under way to address these different behaviors.

IV. Conclusions

We have studied the reaction of thiophene with the $\text{Ti}_8\text{C}_{12}^+$ met-car using density functional theory and tandem-mass spectroscopy. The results presented here are among the first to compare electronic and structural theoretical predictions for the reaction of gas-phase molecules with the Ti_8C_{12} met-car cation with experimental results. The calculations indicate that the Ti_8C_{12} cation adopts a distorted T_d -like structure with no symmetry, similar to what is calculated for the neutral met-car. The sequential addition of thiophene to the $\text{Ti}_8\text{C}_{12}^+$ met-car was calculated and found to be in good agreement with the experimental data. These results illustrate that $\text{Ti}_8\text{C}_{12}^+$ is able to strongly bind up to four thiophene molecules at the low-coordinated Ti^0 sites. DFT calculations further point out the met-car cation withdraws electron density from the adsorbed thiophene. As a result, the stability of the met-car cation increases with an increasing number of bonded thiophene molecules at the Ti^0 sites. This behavior can be contrasted to that on extended metal carbide surfaces whose reactivity decreases with increasing adsorbate coverage. At the same time, the electron density withdrawn from thiophene binding accumulates at the Ti^{I} and the C_2 sites and increases their activity. However, the additional electron density on the $\text{Ti}_8\text{C}_{12}^+$ cation cluster is not sufficient to cleave the C–S bonds of thiophene.

For comparison, calculations were also performed for the reaction between the neutral Ti_8C_{12} met-car and thiophene and reveal a trend in binding energies similar to that observed for the cation. Interestingly, the neutral Ti_8C_{12} , with one extra electron, is found to dissociatively adsorb the first thiophene followed by consecutive addition of intact molecules. While the dissociation products ($\text{S} + \text{C}_4\text{H}_4$) and three intact thiophene molecules bind to the outer Ti^0 sites, the fifth thiophene prefers to share a Ti^0 site with the C_4H_4 hydrocarbon fragment. Despite the initial dissociation and further addition of thiophene molecules, calculations suggest that the reaction to release the adsorbed C_4H_4 into the gas phase is highly activated and is not expected to occur.

Acknowledgment. This research was supported by the U.S. Department of Energy, Division of Chemical Sciences, under contract DE-AC02-98CH10886.

References and Notes

- (1) Guo, B. C.; Kerns, K. P.; Castleman, A. W., Jr. *Science* **1992**, 255, 1411.
- (2) Duncan, M. A. *J. Cluster Sci.* **1997**, 8, 239 and references therein.
- (3) Rohmer, M.-M.; Benard, M.; Poblet, J.-M. *Chem. Rev.* **2000**, 100, 495, and references therein.
- (4) Leswik, B. D.; Castleman, A. W., Jr. *C. R. Physique* **2002**, 3, 251, and references therein.
- (5) Sumathi, R.; Hendrickx, M. *J. Phys. Chem. A* **1998**, 102, 4883.
- (6) Joswick, J.; Springborg, M.; Siefert, G. *Phys. Chem. Chem. Phys.* **2001**, 3, 5130.
- (7) Wang, L. S.; Li, S.; Wu, H. *J. Phys. Chem.* **1996**, 100, 19211.
- (8) Li, S.; Wu, H.; Wang, L. S. *J. Am. Chem. Soc.* **1997**, 119, 7417.
- (9) Sakurai, H.; A. W. Castleman, J. *J. Chem. Phys.* **1999**, 111, 1462.
- (10) Liu, P.; Rodriguez, J. A.; Hua, H.; Muckerman, J. T. *J. Chem. Phys.* **2003**, 118, 7737.
- (11) Hou, H.; Muckerman, J. T.; Liu, P.; Rodriguez, J. A. *J. Phys. Chem. A* **2003**, 107, 9344.
- (12) Gueorguiev, G. K.; Pacheco, J. M. *Phys. Rev. B* **2003**, 68, 241401.
- (13) Gueorguiev, G. K.; Pacheco, J. M. *Phys. Rev. Lett.* **2002**, 88, 115504.
- (14) Liu, P.; Rodriguez, J.; Muckerman, J. T. *J. Phys. Chem. B* **2004**, 108, 18796.
- (15) Lightstone, J. M.; Liu, P.; Patterson, M. J.; White, M. G. *J. Phys. Chem. A* **2006**, in press.
- (16) Chen, J. G. *Chem. Rev.* **1996**, 96, 1477.
- (17) Furimsky, E. *Appl. Catal. A* **2003**, 240, 1.
- (18) Liu, P.; Rodriguez, J. A.; Muckerman, J. T. *J. Phys. Chem. B* **2004**, 108, 15662.
- (19) Liu, P.; Rodriguez, J. A.; Muckerman, J. T. *J. Chem. Phys.* **2004**, 121, 10321.
- (20) Deng, H. T.; Kerns, K. P.; Castleman, A. W. *J. Am. Chem. Soc.* **1996**, 118, 446.
- (21) Guo, B. C.; Kerns, K. P.; A. W. Castleman, J. *J. Am. Chem. Soc.* **1993**, 115, 7415.
- (22) Poblet, J.-M.; Bo, C.; Rohmer, M. M.; Bernard, M. *Chem. Phys. Lett.* **1996**, 260, 577.
- (23) Delley, B. *J. Chem. Phys.* **1990**, 92, 508.
- (24) Delley, B. *J. Chem. Phys.* **2000**, 113, 7756.
- (25) Hammer, B.; Hansen, L. B.; Norskov, J. K. *Phys. Rev. B* **1999**, 59, 7413.
- (26) Baruah, T.; Pederson, M. R.; Lyn, M. L.; A. W. Castleman, J. *Phys. Rev. A* **2002**, 66, 53201.
- (27) Liu, P.; Rodriguez, J. A. *J. Chem. Phys.* **2003**, 119, 10895.
- (28) Rodriguez, J. A.; Liu, P.; Dvorak, J.; Jirsak, T.; Gomes, J.; Takahashi, T.; Nakamura, K. *Phys. Rev. B* **2004**, 69, 115414.
- (29) Baker, J. *J. Comput. Chem.* **1986**, 7, 385.
- (30) Halgren, T. A.; Lipscomb, W. N. *Chem. Phys. Lett.* **1977**, 49, 225.
- (31) Liu, G.; Rodriguez, J. A.; Dvorak, J.; Hrbeck, J.; Jirsak, T. *Surf. Sci.* **2002**, 505, 295.
- (32) Sanchez-Delgado, R. A.; Rosales, M. *Coord. Chem. Rev.* **2000**, 196, 249.
- (33) Rodriguez, J. A.; Dvorak, J.; Jirsak, T. *Surf. Sci.* **2000**, 457, L413.
- (34) Orita, H.; Uchida, K.; Itoh, N. *J. Mol. Catal. A: Chem.* **2003**, 193, 197.